Chapter 3

Surface Oxide–Support Interactions in the Molecular Design of Supported Metal Oxide Selective Oxidation Catalysts

Goutam Deo and Israel E. Wachs

Department of Chemical Engineering, Zettlemoyer Center for Surface Studies, Lehigh University, Bethlehem, PA 18015

A series of metal oxides were deposited on the surface of different oxide supports to study the surface oxide - support interactions. The dehydrated Raman spectra of the supported metal oxide catalysts reveal the presence and structure of the supported metal oxide phases. The same surface metal oxide species were found on the different oxide supports for each of the supported metal oxide systems. The reactivity of the surface metal oxide species, however, depends on the specific oxide support ($TiO_2 \sim ZrO_2 > Nb_2O_5 > Al_2O_3 \sim SiO_2$). For a given oxide support, the reactivity depends on the specific surface metal oxide species (e.g. $VO_x > MoO_y$). The redox activation energy for all the surface metal oxide phases lie in the range of 18-22 kcal/mole. The similar activation energies suggests that the number of active sites and/or the activity per site is responsible for the difference in reactivity. The redox TON for the methanol oxidation reaction correlates with the reduction temperature during TPR experiments, which suggests that the bridging M-O-Support bond controls the activity during redox reactions.

Supported metal oxide catalysts are formed when one metal oxide component (i.e., Re_2O_7, CrO_3, MoO_3, WO_3, V_2O_5, Nb_2O_5, etc.), the supported metal oxide phase, is deposited on a second metal oxide substrate (i.e., Al_2O_3, TiO_2, SiO_2, etc.), the oxide support [1]. The supported metal oxide phase is present on the oxide support as a surface metal oxide species. The reactivity of these

0097–6156/93/0523–0031$06.00/0

supported metal oxide catalysts have been intensively investigated over the past decade in numerous catalytic applications and the main emphasis has been to relate the reactivity with the structure of the surface metal oxide species [1,2]. In determining the structure of these surface metal oxide species Raman spectroscopy has proven to be indispensable because of the ability of Raman spectroscopy to discriminate between different metal oxide species that may simultaneously be present in the catalyst. The reactivity studies have demonstrated that these surface metal oxide species are the active sites for many catalytic reactions [3]. The combined structural and reactivity information currently available about these oxide catalysts is beginning to allow us to develop an understanding of the surface oxide support interactions and to apply this knowledge for the molecular design of supported metal oxide catalysts.

The molecular design of supported metal oxide catalysts requires that we specify the synthesis method, oxide support, catalyst composition, calcination temperature, location of the surface metal oxide species, as well as its reactivity. Consequently, the influence of each of the above parameters upon the structure and catalytic properties of supported metal oxide catalysts needs to be examined. The present study primarily focuses on the molecular design aspects of supported vanadium oxide catalysts because these catalysts constitute a very important class of heterogeneous oxide catalysts. However, comparison with other supported metal oxide systems (MoO_3, Re_2O_7,and CrO_3) will also be made.

Experimental

The oxide supports employed in the present study were: TiO_2 (Degussa, ~55 m^2/g), Al_2O_3 (Harshaw, ~180 m^2/g), SiO_2 (Cabot, ~300 m^2/g), ZrO_2 (Degussa, ~39 m^2/g) and Nb_2O_5 (Niobium Products Co., ~50 m^2/g). Many different synthesis methods have been used to prepare supported metal oxide catalysts. In the case of supported vanadium oxide catalysts, the catalysts were prepared by vapor phase grafting with $VOCl_3$, nonaqueous impregnation (vanadium alkoxides), aqueous impregnation (vanadium oxalate), as well as spontaneous dispersion with crystalline V_2O_5 [4]. No drastic reduction of surface area of the catalysts was observed.

Structural characterization of the surface metal oxide species was obtained by laser Raman spectroscopy under ambient and dehydrated conditions. The laser Raman spectroscope consists of a Spectra Physics Ar^+ laser producing 1-100 mW of power measured at the sample. The scattered radiation was focused into a Spex Triplemate spectrometer coupled to a Princeton Applied Research OMA III optical multichannel analyzer. About 100-200 mg of the pure catalysts were pelletized and used for obtaining the Raman spectra in the dehydrated mode. For ambient spectra 5-20 mg of catalysts was placed on a KBr backing.

The supported metal oxide catalysts were examined for their reactivity in the methanol oxidation reaction. The reactor was operated using milligram amounts of catalysts that provide differential reaction conditions by keeping conversions below 10%. A methanol/oxygen/helium mixture of ~6/13/81 (mole %) at 1 atm pressure was used as the reactant gas for all the data presented. The analysis was performed with an online gas chromatograph (GC) (HP 5840A) containing two columns (Poropak R and Carbosieve SII) and two detectors (FID and TCD). Reaction data at 230 °C are presented in the form of turnover number (TON) - defined as the number of moles of methanol converted per mole of vanadium per second. The reaction data for some catalysts were also obtained at 200, 230, and 240 °C to calculate the activation energy and check for diffusional limitations in the reactor. No mass and heat transfer limitations were observed.

Results and Discussion

The vanadium oxide species is formed on the surface of the oxide support during the preparation of supported vanadium oxide catalysts. This is evident by the consumption of surface hydroxyls (OH) [5] and the structural transformation of the supported metal oxide phase that takes place during hydration-dehydration studies and chemisorption of reactant gas molecules [6]. Recently, a number of studies have shown that the structure of the surface vanadium oxide species depends on the specific conditions that they are observed under. For example, under ambient conditions the surface of the oxide supports possesses a thin layer of moisture which provides an aqueous environment of a certain pH at point of zero charge (pH at pzc) for the surface vanadium oxide species and controls the structure of the vanadium oxide phase [7]. Under reaction conditions (300-500 °C), moisture desorbs from the surface of the oxide support and the vanadium oxide species is forced to directly interact with the oxide support which results in a different structure [8]. These structural transformations taking place during hydration and dehydration conditions of the oxide support suggest that the correlation of the structure - reactivity data should be performed with the structural data obtained under dehydration conditions, and correlating such structural information with the reactivity data.

A series of ~1% V_2O_5 catalysts was prepared by non aqueous impregnation of vanadium tri-isopropoxide oxide (final calcination in oxygen at 450/500 °C) in order to investigate the influence of different oxide supports upon the dehydrated molecular structure and reactivity of the surface vanadium oxide species. Under ambient conditions Raman bands due to orthovanadate, pyrovanadate, metavanadate, and decavanadate species are observed. Assignments of the Raman bands to the different species are made elsewhere [7,9]. At these surface coverages a single surface vanadium oxide species is predominantly present on the different oxide supports as is evident by the presence of a dominant 1015-1039 cm^{-1} band in the dehydrated Raman spectra and potential complication due to additional surface vanadium oxide species are eliminated. The dehydrated Raman band due to the V=O bond was found to vary from 1015-1039 cm^{-1} as a function of the different oxide supports as shown in Figure 1. The slight difference in band position is due to slightly different V=O bond lengths of the isolated surface vanadium oxide species on the different oxide supports and correlates with the different oxygen coordination of the oxide supports. The Raman spectra reveal that essentially the same surface vanadium oxide species is present on all the different oxide supports. This surface vanadium oxide species is described as a distorted four coordinated species possessing a single terminal bond (V=O) and three bonds to the support (V-O-S). The same conclusion is reached from solid state ^{51}V NMR studies of these catalysts [9]. Low surface coverages, ~1% metal oxide, of supported molybdenum oxide (MoO_3) [10], rhenium oxide (Re_2O_7) [11,12], and chromium oxide (CrO_3) [11,12] also indicate the presence of a single surface metal oxide species. The similar Raman band positions of the supported vanadium-oxygen (V=O) stretching frequency during dehydrated conditions are given in Table I. In addition, the structural transformation taking place due to dehydration is observed by comparing columns 2 and 3 of Table I. Thus, at low coverages the dehydrated surface vanadium oxide and related metal oxide molecular structures (Re_2O_7, CrO_3, and MoO_3) are independent of the specific oxide support.

Table I. Dehydrated Raman band position for the V=O terminal stretching vibrations for 1% V_2O_5 on different oxide supports along with the highest ambient Raman band position

Oxide Support	V=O band (cm^{-1}) dehydrated conditions	Highest band (cm^{-1}) ambient conditions
SiO_2	1039	1000
Nb_2O_5	1031	970-980
TiO_2	1027	940-950
ZrO_2	1024	960
Al_2O_3	1015	920-930

The reactivity of the surface vanadium oxide species (~1% V_2O_5) on the different oxide supports was probed by the methanol oxidation reaction. The methanol oxidation reaction is very sensitive to the nature of surface sites present. Surface redox sites form formaldehyde, methyl formate, and dimethoxy methane as the reaction products. Formaldehyde being formed as the first oxidation product from the methoxy intermediate. Subsequent reactions of the methoxy intermediate produces methyl formate and dimethoxy methane. Surface acid sites, Lewis as well as Bronsted, result in the formation of dimethyl ether. Surface basic sites yield CO/CO_2 as the reaction products [9]. For all the supported vanadium oxide catalysts, with the exception of alumina, the surface vanadia redox sites produced formaldehyde almost exclusively. On alumina, only a trace of formaldehyde was formed because the surface acid sites produced dimethyl ether. Thus, for the V_2O_5/Al_2O_3 system the formaldehyde produced was taken as representative of the reactivity of the surface vanadia redox sites. The reactivity of the surface vanadia species on different oxide supports was found to depend dramatically on the specific oxide support as shown in Table II. As the support was changed from silica to zirconia the turnover number (TON) for the surface vanadium oxide species was found to increase by three orders of magnitude. Similar trends were also observed for supported molybdenum oxide [10], rhenium oxide [12], and chromium oxide [12].

Table II. The TON and selectivity to formaldehyde for the methanol oxidation reaction on various 1% supported vanadium oxide catalysts

Oxide Support	TON (sec^{-1})	Selectivity to HCHO (%)
SiO_2	$2.0*10^{-3}$	~80
Al_2O_3	$2.0*10^{-2}$	<1
Nb_2O_5	$7.0*10^{-1}$	~94
TiO_2	$1.8*10^{0}$	~98
ZrO_2	$2.3*10^{0}$	~96

The reactivity of the supported vanadium oxide catalysts for other oxidation reactions also show similar trends as the oxide support is varied from titania to silica [13]. The activity and selectivity for partial oxidation products of vanadium oxide supported on titania being higher than vanadium oxide supported on silica. The oxidation activity of the supported vanadium oxide catalysts is related to the ability to donate oxygen to form the required oxidation products. The origin of this support effect is either due to differences in the terminal V=O bond or the bridging V-O-Support bond. Many publications have proposed that the terminal bond is responsible for catalysis and its activity is directly related to the V=O bond strength [14]. However, comparison of the Raman position of the V=O bond (shorter bond corresponds to higher Raman position) from Table I and TON value for the different supported vanadium oxide catalysts from Table II shows that no relationship exists between the bond strength and activity. A more elaborate analysis of the TON versus bond strength for various supported metal oxide catalysts are performed elsewhere [15]. A more plausible conclusion is that the reactivity is related to the bridging V-O-Support bond since the oxide support has a very significant effect on the reactivity. The trend in reactivity with specific oxide support appears to be related to the surface reducibility of the oxide supports. The more reducible oxide supports (TiO_2, ZrO_2, and Nb_2O_5) always exhibit very high TON while the irreducible oxide supports (Al_2O_3 and SiO_2) always exhibit very low TON [16]. In addition, the importance of the M-O-Support bond during the methanol oxidation reaction suggests that the reactivity should also be a function of the specific supported metal oxide species. Indeed, supported molybdenum oxide catalysts are about one order of magnitude less reactive than supported vanadia catalysts.

Additional information about the reactivity was obtained by determining the kinetic parameters during methanol oxidation for vanadia, molybdena, rhenia, and chromia on different oxide supports. For all these systems the activation energy is approximately the same, 18-22 kcal/mol. The activation energy corresponds to that expected for the breaking of the C-H bond of a surface methoxide intermediate, CH_3O_{ads}, and should be independent of the specific catalyst [17]. The pre-exponential factors, however, vary by orders of magnitude as the oxide support is varied. The similar structures of the supported metal oxide catalysts suggests that the difference in pre-exponential factors is related to either the number of active sites or the activity per site. Irrespective of the exact parameter that affects the pre-exponential factor, it is shown here that the oxide support has a large influence on the reactivity of the surface metal oxide species.

To investigate the effect of the synthesis method on the structure-reactivity relationship of the supported metal oxide catalysts, a series of V_2O_5/TiO_2 catalysts were synthesized by equilibrium adsorption, vanadium oxalate, vanadium alkoxides and vanadium oxychloride grafting [14]. The dehydrated Raman spectra of all these catalysts exhibit a sharp band at ~1030 cm^{-1} characteristic of the isolated surface vanadium oxide species described previously. Reactivity studies with methanol oxidation exhibited similar turnover numbers. Thus, the synthesis method does not affect the final structure or reactivity of the surface vanadium oxide species on titania. Similar conclusions were also found for molybdenum oxide supported on titania [14], silica [18], and alumina [18]. Consequently, the preparation method is not a critical parameter to consider for the design of supported metal oxide catalysts. However, care must be taken to form the surface metal oxide phase without destroying the oxide support or introducing extraneous impurities during preparation.

To study the effect of loading, various amounts of vanadia were deposited on the titania support. The Raman spectra of titania supported vanadia catalysts as a function of vanadia loading reveal the presence of three different vanadia species on the TiO_2 support under dehydration conditions as shown in Figure 2. At low loadings (~1% V_2O_5), a single sharp band is present at ~1027 cm^{-1} which is assigned to an isolated tetrahedral coordinated surface vanadium oxide species containing one terminal V=O bond and three bridging V-O-Ti bonds [19]. At intermediate loadings (2-5% V_2O_5), a second band is present at 920-930 cm^{-1} which has been assigned to a polymerized, tetrahedral coordinated surface vanadium oxide species [19] in addition to the first band at ~1030 cm^{-1}. At high loadings (>6% V_2O_5), a third sharp band is present at 994 cm^{-1} due to crystalline V_2O_5 which indicates that the close-packed surface vanadium oxide monolayer has been formed and all the reactive surface hydroxyls consumed. The first two bands are also present at high loadings. Similar trends in Raman bands are also observed for vanadium oxide supported zirconia, niobia, alumina, and silica and the formation of molecularly dispersed vanadium oxide species always preceeds the formation of crystalline V_2O_5. Thus, the catalyst composition is a critical parameter since it influences the formation of different vanadium oxide structures.

The reactivity of the titania supported vanadium oxide catalysts was probed by the methanol oxidation reaction. The oxidation of methanol over the titania supported vanadia catalysts exclusively yielded formaldehyde, 95%+, as the reaction product. The titania support in the absence of surface vanadia yielded dimethyl ether and trace amounts of CO_2. The almost complete formation of formaldehyde demonstrates that the reactivity of the titania supported vanadia catalysts is due to the surface vanadia redox sites. The turnover numbers of the various vanadia titania catalysts are presented in Table III as a function of the vanadia loading. The TON increases somewhat with initial surface vanadium oxide coverage, and decreases slightly at surface coverages approaching and exceeding monolayer coverage. Note that the TON of bulk V_2O_5 [16] is two orders of magnitude less than the titania supported vanadia catalysts indicating that crystalline V_2O_5 is

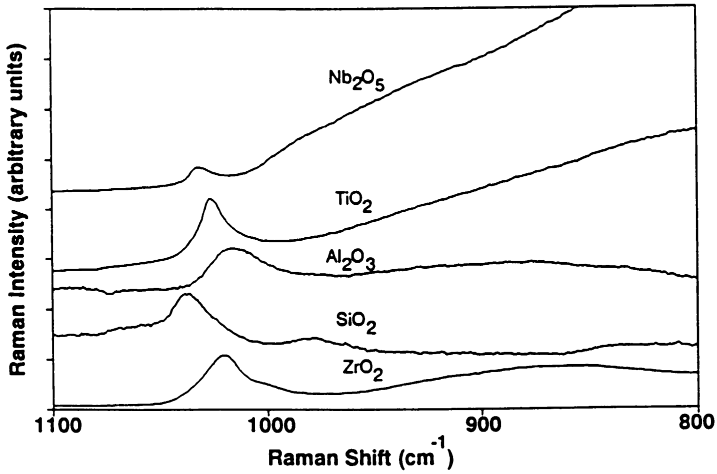

Figure 1. Dehydrated Raman spectra of 1% V_2O_5 on different oxide supports.

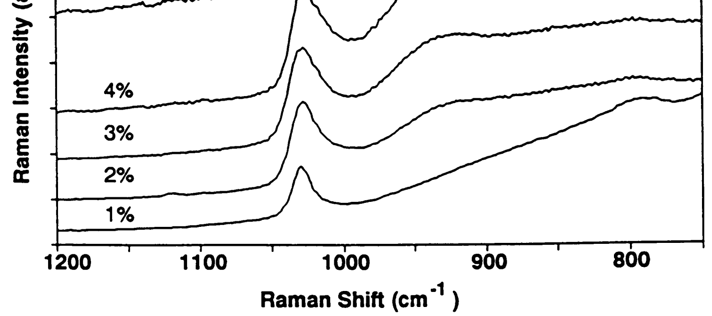

Figure 2. Dehydrated Raman spectra of vanadia-titania catalysts as a function of vanadia loading.

significantly less active than surface vanadia species. The slight increase in TON with increasing surface coverage is not related to the presence of the polymerized surface vanadia species (Raman band at 920-930 cm^{-1}) as the Raman associated with the polymerized species increases continuously up to monolayer coverages and the turnover numbers are comparable. Similar coverage effects were also observed for vanadium oxide supported on zirconia, alumina, and niobia catalysts, as well as for supported rhenium oxide [11], molybdenum oxide [10] and chromium oxide catalysts [12]. Thus, the reactivity of the surface vanadium oxide species essentially does not depend on the surface coverage.

Table III. The TON of V_2O_5/TiO_2 catalysts as a function of loading

wt.% V_2O_5/TiO_2	T.O.N. (sec^{-1})
0.5	1.0
1.0	2.0
2.0	2.7
3.0	1.6
4.0	1.5
5.0	1.3
6.0	1.1
7.0	1.2
bulk V_2O_5	0.022

The nature of the supported vanadium oxide phase is influenced by the calcination temperature. Moderate calcination temperatures, 350-500 °C, are required to decompose the metal oxide precursors (oxalates, alkoxides, oxychlorides, etc.) to form the surface vanadium oxide species [20]. Insufficient calcination temperatures do not completely decompose the precursors and, consequently, the precursors do not react with the surface hydroxyls to form the surface metal oxide species. However, high calcination temperatures, greater than 600 °C, can result in shrinking of the surface area of the oxide support and decreasing the available surface area for the surface metal oxide species. Consequently, high calcination temperatures increase the surface coverage of the metal oxide species and, in severe cases, destroy the surface metal oxide phase and form crystalline V_2O_5 or solid state solutions [7,20]. Thus, calcination temperature is an important parameter that controls the activation and deactivation of supported metal oxide catalysts. However, supported metal oxide catalysts are typically prepared by calcining at 400-500 °C which would eliminate problems with catalyst activation and deactivation.

Typically, the properties of supported metal oxide catalysts are modified by the addition of promoters. To examine the influence of promoters, a series of promoters (tungsten oxide, niobium oxide, silica, potassium oxide and phosphorous oxide) were added to a 1% V_2O_5/TiO_2 catalyst. The influence of the different promoters upon the structure of the surface vanadium oxide species was examined with Raman spectroscopy and the results are presented in Table IV. The addition of monolayer amounts of tungsten oxide and niobium oxide to 1% V_2O_5/TiO_2 catalysts show similar effects observed as the vanadium oxide loading is increased, namely, the appearance of the Raman band at 920-930 cm^{-1}. Monolayer amounts of silica on previously prepared 1% V_2O_5/TiO_2 shows the presence of a single band at 1024 cm^{-1}. In any case the major Raman band is at 1024-1031 cm^{-1} indicating that the vanadium oxide species before and after addition of tungsten oxide, niobium oxide, and silica are structurally similar. However, the addition of potassium oxide and phosphorous oxide had a significant effect on the structure of the surface vanadia species. The addition of potassium oxide decreased the position of the Raman band (corresponding to an increase in V=O bond length), and the addition of phosphorous oxide resulted in the formation of crystalline $VOPO_4$ (major Raman bands at 1038 and 928 cm^{-1} in the 700-1200 cm^{-1} region). The non-interacting promoters (oxides of W, Nb, and Si) did not affect the activity or selectivity of the 1% V_2O_5/TiO_2 catalyst. However, the interacting promoters (potassium oxide and phosphorous oxide) significantly reduced the TON. Thus, promoters that preferentially coordinate to the oxide support (tungsten oxide, niobium oxide and silica) do not affect the structure or reactivity of the surface vanadium oxide species, whereas, promoters that coordinate with the surface vanadia site (phosphorous and potassium) influence the structure and reactivity of the surface vanadia species.

Table IV. Raman band position for promoters on 1% V_2O_5/TiO_2

Promoters on 1% V_2O_5/TiO_2	Raman band positions (700-1200 cm^{-1}) region
None	1027
6% Nb_2O_5	1031, 928
3% SiO_2	1024
7% WO_3	1031, 925
0.3% K_2O	1023, 997
0.7% K_2O	1009, 980
5% P_2O_5	1035, 925

Conclusions

The above discussion demonstrates that it is possible to molecularly design supported metal oxide catalysts with knowledge of the surface oxide - support interactions made possible by the assistance of characterization methods such as Raman spectroscopy and the methanol oxidation reaction. The formation and location of the surface metal oxide species are controlled by the surface hydroxyl chemistry, and the surface metal oxide species are located in the outermost layer of the catalysts as an overlayer. The specific oxide support is a critical parameter since it dramatically affects the reactivity of the surface metal oxide species, even though the surface metal oxide structure is independent of the specific oxide support. The catalyst composition is a critical parameter since it affects the presence of different metal oxide species (isolated surface species, polymerized surface species, and crystalline phases), and the reactivity, TON, is similar for surface metal oxide coverage. The preparation method is not a critical parameter since it does not influence the structure or reactivity of the surface metal oxide species. Calcination temperature is an important parameter that controls activation and deactivation of supported metal oxide catalysts, but calcination temperature is not critical if moderate temperatures, 350-450 °C, are used. Additives that interact with the oxide support do not influence the structure and reactivity of the surface metal oxide species. However, additives that interact with the surface metal oxide do influence the properties of the surface metal oxide species. In summary, the critical parameters that affect the catalytic properties are the specific oxide support, catalyst composition (type of additives) and surface metal oxide coverage.

Acknowledgments

We would like to thank Dr. D.S.Kim, H. Hu, and M. A. Vuurman for their helpful discussions. The financial support by NSF grant # CTS-9006258 is gratefully acknowledged.

Literature Cited

1. (a) Dixit, L.; Gerrard, D. L.; Bowley, H. *Appl. Spectrosc. Rev.* 1986, 22 189.
(b) Bartlett, J. R.; Cooney, R. P. In *Spectroscopy of Inorganic-based Materials*; Clark, R.J.H. and Hester, R.E., Eds; Wiley: New York, 1987; pp 187.
(c) Hardcastle, F.D.; Wachs, I. E. In *Proc. 9th Intern. Congr. Catal.*; Phillips, M.S. and Ternan, M., Eds., Chemical Institute of Canada, Ontario, 1988, Vol. 4; pp 1449.
2. Wachs, I. E. *Chem. Eng. Sc.* 1990, 45(8), 2561.

3. Bond, G. C.; Tahir, S. F. *Appl. Catal.* 1991, 71, 1.
4. Machej, T.; Haber, J.; Turek, A. M.; Wachs, I. E. *Appl. Catal.* 1991, 70, 115.
5. (a) Segawa, K.; Hall, W.K. *J. Catal.* 1982, 77, 221.
   (b) Kim, D. S.; Kurusu, Y.; Segawa, K.; Wachs, I. E. In *Proc. 9th Inter. Congr. Catal.*; Phillips, M.S. and Ternan, M., Eds., Chemical Institute Canada, Ontario, 1988, Vol. 4, pp 1460.
   (c) Turek, A. M.; Wachs, I. E.; Decanio, E. *J. Phys. Chem* 1992, 96, 5000.
6. (a) Went, G. T.; Oyama, S. T.; Bell, A. T. *J. Phys. Chem.* 1990, 94, 4240.
   (b) Vuurman, M. A.; Wachs, I. E.; Hirt, A. M. *J. Phys. Chem.* 1991, 95, 9928.
7. Deo, G.; Wachs, I. E. *J. Phys. Chem.* 1991, 95, 5889.
8. (a) Anpo, M.; Tanahashi, I.; Kubokawa, Y. *J. Phys. Chem.* 1980, 84, 3440.
   (b) Cristiani, C.; Forzatti, P.; Busca, G. *J. Catal.* 1991, 116, 586.
9. (a) Eckert, H.; Wachs, I. E. *J. Phys. Chem.* 1989, 93, 6796.
   (b) Eckert, H.; Deo, G.; Wachs, I. E., unpublished results.
10. Hu, H.; Wachs, I. E., in preparation.
11. Vuurman, M. A.; Wachs, I. E.; Stufkens, D.J.; Oskam, A. *J. Mol. Catal.*, 1992, in press.
12. Kim, D. S.; Wachs, I. E. *J. Catal.* 1992, in press.
13. (a) Wainwright, M. S.; Foster, N. R. *Catal. Rev.* 1979, 19, 211.
    (b) Hauffe, K.; Raveling, H. *Ber. Bunsenges. phy. Chem.* 1980, 84, 912.
14. Klissurski, D.; Abadzhijeva, N. *React. Kinet. Catal. Lett.* 1975, 2, 431.
15. Wachs, I. E.; Deo, G.; Kim, D. S.; Vuurman, M. A.; Hu, H. In *Preprints of the Proceedings of the 10th Internation Congress of Catalysis*, 1992, 72.
16. Deo, G.; Wachs, I.E. *J. Catal.* 1991, 129, 307.
17. (a) Yang, T. S.; Lunsford, J. H. *J. Catal.* 1987, 103, 55.
    (b) Fareneth, W. E.; Ohuchi, F.; Staley, R. H.; Chowdhry, U.; Sleight, A. W. *J. Phys. Chem.* 1985, 89, 2493.
18. (a) Williams, C. C.; Ekerdt, J. G.; Jehng, J.-M.; Hardcastle, F. D.; Turek, A. M.; Wachs, I. E. *J. Phys. Chem.* 1991, 95, 8781.
    (b) Williams, C. C.; Ekerdt, J. G.; Jehng, J.-M.; Hardcastle, F. D.; Wachs, I. E. *J. Phys. Chem.* 1991, 95, 8791.
19. Wachs, I. E. *J. Catal.* 1990, 124, 570.
20. Saleh, R. Y.; Wachs, I. E.; Chan, S. S.; Chersich, C. C. *J. Catal.* 1986, 98, 102.

RECEIVED October 30, 1992